Proceedings of the 21st ICSMGE, Vienna, Austria, 14 – 19 June 2026. Pistrol, Adam & Schweiger (eds.)
Published by: ÖGG, Austrian Society for Geomechanics, Salzburg, Austria, ISBN 978-3-9503898-4-5
https://doi.org/10.53243/ICSMGE2026-1639

A non-isothermal cavity expansion analytical model for the analysis of energy tunnels

Arianna Lupattelli, Diana Salciarini
Department of Civil and Environmental Engineering, University of Perugia, Via G. Duranti 93, 06125 Perugia, Italy

Alessandro F. Rotta Loria
Subsurface Opportunities and Innovations Laboratory (SOIL), Department of Civil and Environmental Engineering, Northwestern University, 2145 Sheridan Road, Evanston, IL 60208, USA

ABSTRACT: Energy tunnels represent an innovative solution for harnessing clean and renewable energy in urban environments, combining tunneling infrastructure with ground-source heat exchange systems. While numerous numerical approaches have been proposed by various authors to analyze the thermo-mechanical behavior of energy tunnels, simplified analytical models—widely available for other types of energy geostructures—are still lacking in this context. Such models can play a crucial role in the early design stages by offering quick evaluations of thermally induced stresses and strains, and can be applied more broadly to problems involving cylindrical cavity-type geometries. The proposed analytical approach accounts for thermal fluctuations in the elastic stress and strain fields, under both steady-state and time-dependent thermal conditions. Validation through finite element simulations targeting medium-temperature applications confirmed the models' ability to predict the mechanical response of energy tunnels by capturing thermally induced stresses and strains, which can be superimposed at any stage onto those caused by conventional mechanical loads. Although specifically developed with energy tunnels in mind, the formulation is broadly applicable to a wide range of geotechnical problems involving circular cavities. This work lays the foundation for future developments to enhance the model's applicability to real-world scenarios.

KEYWORDS: Energy tunnels, cylindrical cavities, analytical model, non-isothermal cavity expansion, FE validation analysis.

1 INTRODUCTION

Energy geostructures (EGs)—including energy piles, walls, slabs, and tunnels—combine the structural support functions of traditional geotechnical elements with the ability to exchange thermal energy with the ground. This dual role enables the exploitation of low-enthalpy geothermal energy in a sustainable and space-efficient manner, particularly within dense urban environments.

Over the past two decades, considerable research efforts have focused on advancing the understanding and modeling of EGs. Numerical models of varying complexity have been widely employed to investigate their thermo-mechanical behavior, with particular focus on energy piles (e.g., Laloui et al. 2006; Batini et al. 2015; Lupattelli & Salciarini 2025), energy tunnels (e.g., Barla et al. 2018; Rotta Loria et al. 2022), and energy walls (e.g., Sterpi et al. 2017; Dai et al. 2022). These models have progressively improved, benefiting from advances in computational resources and providing valuable insights into the multiphysical processes involved in EG operation. However, despite the growing accessibility of numerical modeling in academic research, such approaches often remain challenging for routine engineering practice. The need for specialized expertise, long computational times, and complex coupling schemes can hinder their practical application in everyday design workflows.

As a result, analytical models remain a crucial tool for the preliminary analysis and design of EGs, offering efficiency and transparency based on sound theoretical principles, particularly when numerical methods prove too complex or computationally demanding for practical engineering use. For energy piles and walls in particular, a range of analytical formulations has been developed to describe their response to combined thermal and mechanical loading conditions (e.g., Rotta Loria & Laloui 2017; Sterpi et al. 2017; Laloui & Rotta Loria 2019; Zannin et al. 2020; Loveridge et al. 2020; Dai et al. 2022). By contrast, the study of energy tunnels (ETs) has largely relied on full-scale monitoring and advanced numerical modeling, often involving fully coupled thermo-hydro-mechanical simulations (e.g., Barla et al. 2016; Ma et al. 2022).

Despite these approaches offer detailed insights into ET behavior, they are resource-demanding and rarely accessible for routine engineering use.

At present, there is no analytical model in the literature capable of predicting thermally induced stresses and deformations around geostructures with cylindrical cavity-type geometries. This lack of analytical models for ETs represents a critical gap, especially considering their availability for other EGs. Such models are essential for early-stage design and parametric analyses, and their absence hampers both practical application and theoretical development.

To address this shortcoming, the present work proposes a simplified analytical model to describe the thermo-mechanical response of cylindrical cavities in soil under thermal loading—laying the groundwork for future analytical approaches to ETs. The model is rooted in classical *cavity expansion theory* (*CET*), a fundamental concept in theoretical geomechanics widely used to describe the mechanical behavior of cylindrical cavities in elastic or elasto-plastic media (Yu, 2000). Here, *CET* is extended to include non-isothermal conditions, accounting for the thermal stresses and strains generated during heat injection. The model is finally validated against finite element simulations in steady-state and transient thermal conditions.

2 ANALYTICAL FRAMEWORK

2.1 *Non-isothermal cavity expansion theory*

The system consists of a cylindrical cavity characterized by internal and external radii r_a and r_b, respectively. The cavity is initially subjected to a uniform temperature T_0, while the internal and external horizontal pressures p and p_0, respectively, are assumed to be zero at the initial state (Figure 1).

This problem has a well-established solution, which can be found in classical references such as Timoshenko & Goodier (1951). The surrounding soil is modeled as a homogeneous, isotropic elastic medium, characterized by Young's modulus E, and Poisson's ratio ν. During the thermal process, a fixed temperature T_a, higher than T_0, is applied on the inner surface of the cavity. This thermal load induces a gradual internal pressure increase, causing the cylindrical cavity to expand.

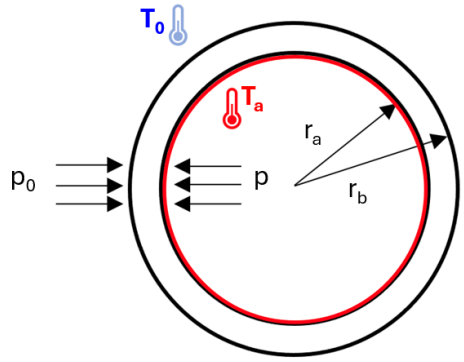

Figure 1. Cylindrical cavity subjected to uniform internal and external pressures, with temperature applied on the inner surface.

The problem is formulated in cylindrical polar coordinates (r,θ,z), and the analysis is carried out under plane strain conditions, implying no dependence on the vertical coordinate, z, thus treating the radial, r and hoop, θ directions as the principal directions.

The equilibrium equation in cylindrical coordinates can be expressed in terms of radial and hoop stresses as follows:

$$r\frac{d\sigma_r}{dr} + (\sigma_r - \sigma_\theta) = 0 \tag{1}$$

where σ_r and σ_θ are the normal stresses acting in the radial and tangential directions, respectively. The radial stress is known on both internal and external boundaries, and can be written as:

$$\begin{cases} \sigma_r = p, & r = r_a \\ \sigma_r = p_0, & r = r_b \end{cases} \tag{2}$$

Corresponding to the radial and hoop stresses, there are two normal strain components in the same directions that can be expressed in Equations (3) and (4) as functions of the radial displacement u:

$$\varepsilon_r = -\frac{du}{dr} \tag{3}$$

$$\varepsilon_\theta = -\frac{u}{r} \tag{4}$$

while Equation (5) can be used to eliminate the displacement u to give the compatibility condition:

$$\varepsilon_r = \frac{d}{dr}(r\varepsilon_\theta) \tag{5}$$

Compared to the conventional model, the difference lies in the additional contribution of the temperature effect within the material constitutive equation, which considers the additional strain produced by changes of temperature. This strain contribution has inherently a dilative nature (thermal expansion) and does not cause any shear, and it is proportional to temperature changes. With respect to the classical cavity expansion formulation, material elasticity is replaced by the thermo-elastic relationship, according to Forte et al. (2019). Here, the total strain at each point of a material characterized by a thermo-elastic behavior is generally given by the sum of two contributions. The former includes the strain induced by the application of a stress field that is required to maintain the continuity of the material (generalized *Hooke's law*). The latter includes the strain induced by the application of a temperature change to the material. These considerations can be mathematically expressed as:

$$\sigma_r = 2\mu\varepsilon_r + \lambda(\varepsilon_r + \varepsilon_\theta) + kT \tag{6}$$

$$\sigma_\theta = 2\mu\varepsilon_\theta + \lambda(\varepsilon_r + \varepsilon_\theta) + kT \tag{7}$$

with μ, λ, and k the elastic coefficients. Equation (6) and (7) can be rewritten by explicitly expressing the radial and hoop strains in terms of stresses as:

$$\varepsilon_r = \frac{1-\nu^2}{E}\left[\sigma_r - \frac{\nu}{1-\nu}\sigma_\theta - \frac{E\alpha T}{1-\nu}\right] \tag{8}$$

$$\varepsilon_\theta = \frac{1-\nu^2}{E}\left[\frac{\nu}{1-\nu}\sigma_r + \sigma_\theta - \frac{E\alpha T}{1-\nu}\right] \tag{9}$$

where α is the linear thermal expansion coefficient, and T the temperature distribution function.

2.2 *Temperature distribution*

The term T appearing in Equations (8) and (9) denotes the temperature distribution within the cavity along the radial direction. Its formulation depends on the thermal regime under consideration: in the case of a steady-state analysis, it is expressed as T_r, whereas for a time-dependent (transient) analysis, it is expressed as $T_{r,t}$, due to the explicit dependence on time.

Under steady-state conditions without internal heat generation (Bergman, 2011), the heat conduction equation simplifies and can be solved, assuming constant thermal conductivity k, to obtain the temperature distribution within a hollow cylinder. By integrating the equation twice and applying the boundary conditions:

$$\begin{cases} T_r = T_a, & r = r_a \\ T_r = T_b, & r = r_b \end{cases} \tag{10}$$

the integration constants are determined. Substituting these into the general solution yields the temperature profile T_r, along the radial direction, resulting from the temperature increase inside the cavity as expressed in Equation (11):

$$T_r = \frac{T_a - T_0}{\ln(r_a) - \ln(r_b)}\ln(r) - \ln(r_b) + T_0 \tag{11}$$

Time-dependent (transient) heating occurs when the temperature or boundary conditions of a system change over time, causing the temperature field within the material to evolve until it eventually reaches a steady state. The temperature distribution $T_{r,t}$ at any time is obtained by solving the transient heat conduction equation in cylindrical coordinates (Bergman, 2011). According to Luikov (1968), the solution can be expressed as a sum of a steady-state term and a transient component $\theta_{r,t}$ as expressed in Equation (12):

$$T_{r,t} = T_r + \vartheta_{r,t} \tag{12}$$

The transient component is expanded in Bessel functions as:

$$\vartheta_{r,t} = T_i\left[\pi\sum_{n=1}^{\infty}\exp(-\lambda_n^2 Fo)\frac{J_0(a_n)U_0(R\lambda_n)}{J_0(a_n)+J_0(b_n)}\right] \tag{13}$$

$$-\left[\pi\frac{T_b}{T_i}\sum_{n=1}^{\infty}\frac{(J_0(a_n)-T_iJ_0(b_n))J_0(a_n)U_0(R\lambda_n)}{J_0^2(a_n)-J_0^2(b_n)}\exp(-\lambda_n^2 Fo)\right] \tag{10}$$

where: T_i is the ratio of the temperatures at the inner radius T_a, to the outer one T_b; R is the ratio of the outer radius r_b, to the generic radial position r; R_i is the ratio of the inner radius r_a, to the outer radius r_b; Fo is the Fourier number; J_0 and Y_0 are the Bessel function of the first and second kind of zero order, respectively; U_0 is the characteristic equation; λ_n are the roots determined from the characteristic equation (*eigenvalues*); a_n is

defined as the product of R_i and λ_n; b_n corresponds to the eigenvalue λ_n.

3 ANALYTICAL MODEL FORMULATION

With the aim of deriving expressions for the radial and hoop stresses (σ_r and σ_θ), deformations (ε_r and ε_θ), and radial displacements (u_r) within a generic cylindrical cavity, the equilibrium and the thermo-elasticity constitutive law are incorporated into the compatibility equation, resulting in:

$$\frac{1-\nu^2}{E}\left\{\sigma_r - \frac{\nu}{1-\nu}\left[\sigma_r + \frac{r d\sigma_r}{dr}\right] - \frac{E\alpha T}{1-\nu}\right\} = \frac{d}{dr} r\left\{\frac{1-\nu^2}{E}\left[\sigma_r + r\frac{d\sigma_r}{dr} - \frac{\nu}{1-\nu}\sigma_r - -\frac{E\alpha T}{1-\nu}\right]\right\} \tag{14}$$

leading to the second-order differential equation:

$$r\frac{d^2\sigma_r}{dr^2} + 3\frac{d\sigma_r}{dr} + \frac{E\alpha}{1-\nu}\frac{dT}{dr} \tag{15}$$

At this stage, depending on whether the problem is steady-state or time-dependent, the appropriate expression for the temperature will be substituted into the formulation.

3.1 *Steady-state condition*

By integrating Equation (15), the expression of the radial stress has the following general solution:

$$\sigma_r = \frac{E\alpha}{2(1-\nu)}\frac{\ln(r)}{\ln(r_a) - ln(r_b)} - \frac{C}{r^2} + D \tag{16}$$

where ΔT is the difference between the inner temperature of the cavity T_a and the initial temperature T_0, while C and D are integration constants. By substituting Equation (16) into Equation (1), the following expression for the hoop stress is obtained:

$$\sigma_\theta = \frac{E\alpha}{2(1-\nu)}\frac{\ln(r)+1}{\ln(r_a) - ln(r_b)} + \frac{C}{r^2} + D \tag{17}$$

Applying the same mechanical boundary conditions written in Equation (10) to Equations (16) and (17), the integration constants C and D are defined as follows:

$$C = \frac{r_a^2 r_b^2}{r_b^2 - r_a^2}\left[\frac{E\alpha\Delta T}{2(1-\nu)} + p_0 - p\right] \tag{18}$$

$$D = \frac{r_b^2 p_0 - r_a^2 p}{r_b^2 - r_a^2} + \frac{E\alpha\Delta T}{2(1-\nu)}\left[\frac{r_b^2}{r_b^2 - r_a^2}\frac{\ln(r_a)}{\ln(r_a) - ln(r_b)}\right] \tag{19}$$

By substituting the integration constants into the Equations (16) and (17), the following expressions for the thermally induced radial and hoop stresses are obtained:

$$\sigma_r = \frac{E\alpha\Delta T}{2(1-\nu)}\left[\frac{\ln(r) - \ln(r_a)}{\ln(r_a) - ln(r_b)} + \frac{r_b^2(r^2 - r_a^2)}{r^2(r_b^2 - r_a^2)}\right] + \frac{p r_a^2(r_b^2 - r^2)}{r^2(r_b^2 - r_a^2)} + \frac{p_0 r_b^2(r^2 - r_a^2)}{r^2(r_b^2 - r_a^2)} \tag{20}$$

$$\sigma_\theta = \frac{E\alpha\Delta T}{2(1-\nu)}\left[\frac{\ln(r) - \ln(r_a) + 1}{\ln(r_a) - ln(r_b)} + \frac{r_b^2(r^2 - r_a^2)}{r^2(r_b^2 - r_a^2)}\right] - \frac{p r_a^2(r_b^2 + r^2)}{r^2(r_b^2 - r_a^2)} + \frac{p_0 r_b^2(r^2 + r_a^2)}{r^2(r_b^2 - r_a^2)} \tag{21}$$

Based on the expressions of stresses (σ_r and σ_θ), radial and hoop strains ε_r and ε_θ, can be expressed by substituting Equations (20) and (21) into Equations (8) and (9), while the radial displacement u_r can be determined from Equation (4).

3.2 *Time-dependent condition*

Equation (15) was implemented numerically in MATLAB. The code used in this study solves a thermo-elastic boundary value problem by formulating it as an ordinary differential equation (ODE), describing how a physical quantity varies with respect to a single independent variable by relating it to its derivatives. In this context, the unknown quantity is the radial stress distribution $\sigma_{r,t}$, which is not available in closed form but is governed by its spatial variation. The governing differential equation obtained from the radial equilibrium condition in cylindrical coordinates, combined with the linear thermo-elastic constitutive laws, includes the effect of a non-uniform temperature field. To enable numerical its integration, Equation (15) is converted from the original second-order equation into a first-order ODEs using the auxiliary variables:

$$y_1 = \sigma_{r,t} \tag{22}$$

$$y_2 = \frac{d\sigma_{r,t}}{dr} \tag{23}$$

leading to an equivalent system:

$$\begin{cases} y_1' = y_2 \\ y_2' = \dfrac{E\alpha}{1-\nu}\dfrac{dT}{dr} - \dfrac{3}{r}y_2 \end{cases} \tag{24}$$

This system is then solved using MATLAB's *bvp4c* routine, which is designed to handle boundary value problems for ODEs. The imposed boundary conditions require the radial stress to vanish at both the internal and external surfaces:

$$\begin{cases} \sigma_{r,t}(r_a, t) = 0, \\ \sigma_{r,t}(r_b, t) = 0, \end{cases} \tag{25}$$

The final solution obtained from the solver provides $\sigma_{r,t}$ in a discrete numerical form over a radial mesh and corresponds to the solution of the boundary value problem in Equation (26):

$$\sigma_{r,t} = -\frac{1}{r^2}\int_{r_a}^{r}\left[\int_{r_a}^{\rho}\rho'^2\frac{E\alpha}{1-\nu}\frac{dT}{dr}(\rho', t)d\rho'\right]\frac{d\rho}{\rho} + C + \frac{D}{r^2} \tag{26}$$

Here, ρ and ρ' are integration variables introduced to express the differential equation in a closed-form integral representation:

- ρ' is the inner variable of integration, representing the radial position where the thermal gradient contributes to the accumulation of thermal strain.
- ρ is the outer variable, running from r_a to r, used to construct the solution for the second derivative of $\sigma_{r,t}$.

The integration constants C and D are determined by enforcing the boundary conditions in Equation (25).

The final solution obtained via *bvp4c* does not have a closed-form analytical expression, since the differential equation involves the term *dT/dr*, which depends on a numerical solution of the heat conduction problem (obtained using Bessel functions). The solver computes a numerically stable and differentiable approximation of $\sigma_{r,t}$ across a discretized radial domain, satisfying both the differential system and the boundary conditions within the specified tolerances. Consequently, $\sigma_{r,t}$ is also obtained numerically. The resulting function is subsequently used to compute the hoop

stress $\sigma_{\theta,t}$, radial and hoop strains $\varepsilon_{r,t}$ and $\varepsilon_{\theta,t}$, and displacements $u_{r,t}$ according to Equations (1), (8), (9) and (4), respectively.

4 COMPARISON WITH 2D FEM

Comparative finite element analyses were conducted using the COMSOL Multiphysics numerical code to validate the new analytical models derived from the conventional *CET*, which incorporates a thermal module accounting for the additional stresses and strains in a generic cylindrical cavity

A two-dimensional (2D) plane-strain model with the analysis plane oriented normally to the cavity's axis has been established for the cylindrical cavity. Due to the symmetry of the problem, only a quarter is analyzed, as shown in Figure 2.

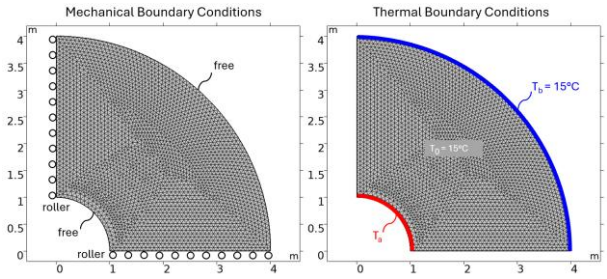

Figure 2. Domain geometry, mesh and thermo-mechanical boundary conditions.

The cavity has a radius r_a of 1 m, while the outer boundary is set to r_b = 4 m. The left and bottom boundaries of the domain, representing the axis of symmetry, are subject to roller boundary conditions. These assumptions have been commonly employed in previous models of EGs (Batini et al. 2015; Cousin et al. 2019; Rotta Loria, 2021; Kong et al. 2023). The inner and outer cavity boundaries are free to move, without pressure boundary conditions (p=p_0=0). The elastic material parameters characterizing the domain are reported in Table 1, referring to Rotta Loria (2021).

Table 1. Material properties adopted in the simulations (Rotta Loria, 2021).

Parameter	Symbol	Value	Unit
Specific weight	ρ_{soil}	1963	kg/m^3
Young's modulus, soil	E_{soil}	134	MPa
Young's modulus, concrete	$E_{concrete}$	30000	MPa
Poisson's ratio	ν_{soil}	0.3	-
Specific heat capacity	$C_{p,soil}$	1157	J/Kg·K
Thermal conductivity	k_{soil}	2.10	W/m·K

To better reproduce the typical configuration of an ET, which includes the presence of a concrete lining, an equivalent Young's modulus E_{eq}, has been adopted for the entire domain, taking into account the thickness of the lining, as well as the surrounding soil, using the elastic Lamè constant λ, expressed as:

$$\lambda = \frac{E_{concrete}}{G_{soil}} \tag{27}$$

The equivalent Young's modulus, E_{eq}, was estimated assuming three different values both for the Lamè constant and for the Poisson's ratio, following the equation:

$$E_{eq} = \frac{2(1+\nu_{soil})E_{concrete}}{\lambda} \tag{28}$$

To validate the results of the numerical model with the analytical model developed based on the non-isothermal *CET* formulation implemented with thermal contributions, a sensitivity analysis has been conducted. The variation of the following parameters has been considered, as detailed in Table 2: stiffness parameters λ and ν; linear thermal expansion coefficient α_{soil}; inner temperature boundary T_a.

Table 2. Description of the values used for conducting the sensitivity analysis.

Parameter	Parametric values	Unit
Lamè constant, λ	100–1000–1000	-
Poisson's ratio, ν_{soil}	0.2–0.3–0.45	-
Linear thermal expansion, α_{soil}	1E^{-5}–1E^{-6}–1E^{-7}	1/°C
Temperature, T_a	25–30–40	°C

4.1 *Results*

A comparison between the numerical and analytical approaches for the non-isothermal *CET* model is illustrated in Figure 3, Figure 4, Figure 5 and Figure 6, based on a sensitivity analysis involving the variation of the parameters reported in Table 3. The results are expressed in terms of radial and hoop stresses and strains, as well as displacements. Due to space constraints, only a representative subset of the resulting plots is presented herein.

In the steady-state regime, the influence of thermal loading is investigated through the distribution of stress and strain components. Figure 3 presents the radial and hoop stress fields induced by thermal effects, showing the sensitivity of the stress response to variations in the equivalent Young's modulus E_{eq} of the lining material, resulting from the variation of the Lamé constant λ.

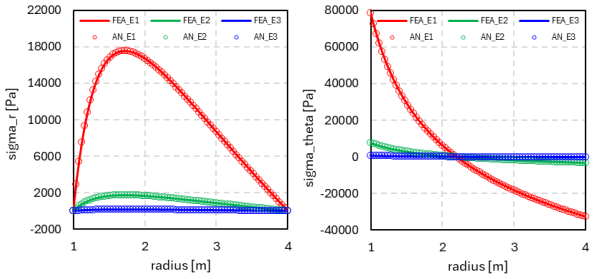

Figure 3. Comparison of steady-state non-isothermal analysis results between the finite element model (solid line) and the analytical model (circles). E_{eq} related to the lining covering the cavity varies for three values of λ: E_{eq1} = 7.8E^8 Pa, E_{eq2} = 7.8E^7 Pa, and E_{eq3} = 7.8E^6 Pa.

In contrast, Figure 4 illustrates the thermally induced radial and tangential strains, highlighting the deformation behavior of the system under different temperatures applied at the cavity inner boundary. These results underline the coupling between thermal loading and mechanical response in the steady state, where both material stiffness and boundary temperature play a significant role.

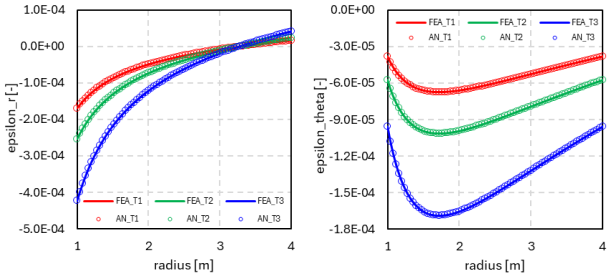

Figure 4. Comparison of steady-state non-isothermal analysis results between the finite element model (solid line) and the analytical model (circles). T applied to the inner boundary of the cavity varies for three values: $T_1 = 25°C$, $T_2 = 30°C$, and $T_3 = 40°C$.

The time-dependent analysis, evaluated after one year, further explores the evolution of thermo-mechanical behavior. Figure 5 shows the variation in radial stress and displacement as a function of E_{eq}, resulting from the variation of the Poisson's ratio ν_{soil}, emphasizing how increased stiffness amplifies both stress development and radial displacements over time.

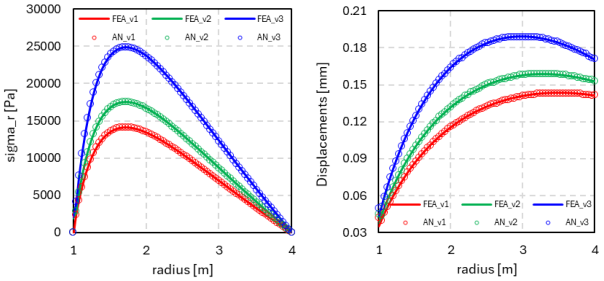

Figure 5. Comparison of time-dependent non-isothermal analysis (after 1 year) results between the finite element model (solid line) and the analytical model (circles). E_{eq} related to the lining covering the cavity varies for three values of ν_{soil}: $E_{eq1} = 7.8E^8$ Pa, $E_{eq2} = 7.8E^7$ Pa, and $E_{eq3} = 7.8E^6$ Pa.

Figure 6, on the other hand, focuses on the impact of thermal expansion. It displays the radial stress and radial strain distributions resulting from different values of the linear thermal expansion coefficient α_{soil}, underscoring the critical role of this parameter in long-term thermally induced deformations.

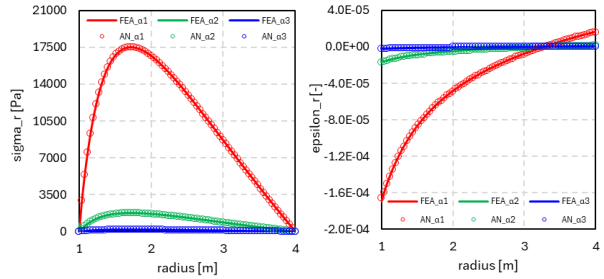

Figure 6. Comparison of time-dependent non-isothermal analysis (after 1 year) results between the finite element model (solid line) and the analytical model (circles). The linear thermal expansion of soil varies for three values: $\alpha_{soil1} = 1E^{-5}$ 1/°C, $\alpha_{soil2} = 1E^{-5}$ 1/°C, and $\alpha_{soil3} = 1E^{-5}$ 1/°C.

5 CONCLUSIONS

This work introduces a new analytical formulation that extends the classical cavity expansion theory by incorporating a thermo-elastic component, accounting for both steady-state and time-dependent thermal effects. The aim was to quantify the impact of temperature fluctuations on the stress and strain distributions around a generic cylindrical cavity into a uniform material medium.

The results confirm the validity and applicability of the proposed model in various soil mechanics contexts involving cavity geometries. A particularly relevant application is in energy tunnels, which integrate ground-source heat exchange systems to facilitate thermal energy transfer between the ground and the surrounding environment. In this context, the proposed formulation offers a practical tool for engineers and researchers, effectively translating theoretical insights into solutions for complex geotechnical challenges related to sustainable urban infrastructure.

This study marks an important step toward establishing a more comprehensive analytical framework for the analysis of energy tunnels, addressing a key gap in the existing literature and offering a viable alternative to more complex numerical models.

6 REFERENCES

Laloui, L., Nuth, M., and Vulliet, L. 2006. Experimental and Numerical Investigations of the Behavior of a Heat Exchanger Pile. *International Journal for Numerical and Analytical Methods in Geomechanics* 30(8), 763-781.

Batini, N., Rotta Loria, A.F., Conti, P., Testi, D., Grassi, W., and Laloui, L. 2015. Energy and geotechnical behaviour of energy piles for different design solutions. *Applied Thermal Engineering* 86, 199-213.

Lupattelli, A., and Salciarini, D. 2025. Investigating the impact of temperature recovery across different thermal activation scenarios of a real-world energy piled foundation. *Tunnelling and Underground Space Technology* 158, 106457.

Barla, M., and Di Donna, A. 2018. Energy tunnels: concept and design aspects. *Underground Space* 3(4), 268-276.

Rotta Loria, A.F., Di Donna, A., and Zhang, M. 2022. Stresses and deformations induced by geothermal operations of energy tunnels. *Tunnelling and Underground Space Technology* 124, 104438.

Sterpi, D., Coletto, A., and Mauri, L. 2017. Investigation on the behaviour of a thermo-active diaphragm wall by thermo-mechanical analyses. *Geomechanics for Energy and the Environment* 9, 1-20.

Dai, Q., Rotta Loria, A.F., and Choo, J. 2022. Effects of internal airflows on the heat exchange potential and mechanics of energy walls. *Renewable Energy* 197, 1069-1080.

Rotta Loria, A.F., and Laloui, L. 2017. The equivalent pier method for energy pile groups. *Géotechnique* 67, 691-702.

Laloui, L., and Rotta Loria, A.F. 2019. *Analysis and Design of Energy Geostructures: Theoretical Essentials and Practical Application*. Cambridge: Academic Press.

Zannin, J., Rotta Loria, A.F., Labjani, Q., and Laloui, L. 2020. Extension of Winkler's solution to nonisothermal conditions for capturing the behaviour of plane geostructures subjected to thermal and mechanical actions. *Computers and Geotechnics* 128, 103618.

Loveridge, F., McCartney, J.S., Narsilio, G., and Sanchez, M. 2020. A review of analysis approaches, in situ testing and model scale experiments. *Geomechanics for Energy and the Environment* 22, 100173.

Barla, M., Di Donna, A., and Perino, A. 2016. Application of energy tunnels to an urban environment. *Geothermics* 61, 104-113.

Ma, C., Di Donna, A., and Dias, D. 2022. Numerical study on the thermo-hydro-mechanical behaviour of an energy tunnel in a coarse soil. *Computers and Geotechnics* 151, 105003.

Yu, H. 2000. *Cavity Expansion Methods in Geomechanics*. Dordrecht: Springer-Science+Business Media, B.Y.

Timoshenko, S., and Goodier, J. (1951). *Theory of Elasticity*. 3rd Edition. New York: McGraw-Hill.

Forte, S., Preziosi, L., and Vianello, M. 2019. *Meccanica dei Continui*. Milan: Springer-Milano.

Bergman, T.L. 2011. *Fundamentals of Heat and Mass Transfer*. 7th Edition. Jefferson City: John Wiley & Sons, Inc.

Luikov, A.V. 1968. Analytical heat diffusion theory. London: Academic Press, Inc.

Cousin, B., Rotta Loria, A., Bourget, A., Rognon, F., and Laloui, L. 2019. Energy performance and economic feasibility of energy segmental linings for subway tunnels. *Tunnelling and Underground Space Technology* 91, 102997.

Rotta Loria, A. 2021. The thermal energy storage potential of underground tunnels used as heat exchangers. *Renewable Energy* 176, 214-227.

Kong, G., Wu, D., and Wei, Y. 2023. Experimental and numerical investigations on the energy and structural performance of a full-scale energy utility tunnel. *Tunnelling and Underground Space Technology* 139, 105208.